APPENDIX A
HYBRID *ac/dc*-MICROGRID TOPOLOGY

The configuration of the HMG used to validate the performance of the proposed control strategy is shown in Fig. A1, where the circuit parameters are given in Table A1, and the parameters of the controllers are given in Table A2. The simulated system is composed of fifteen units: six *ac*-DGs composing the *ac*-MG, six *dc*-DGs composing the *dc*-MG, and three *ICs* for interconnecting the *ac*-MG and the *dc*-MG. The nominal voltage in the *ac*-MG is 415V@50Hz (phase-to-phase RMS voltage), while in the *dc*-MG the nominal voltage is 400V. The generation cost functions of DG units are assumed quadratic (i.e., $C_{\mathrm{ac}-i}(P^{\mathrm{G}}_{\mathrm{ac}-i}) = a_{\mathrm{ac}-i}(P^{\mathrm{G}}_{\mathrm{ac}-i})^2 + b_{\mathrm{ac}-i}P^{\mathrm{G}}_{\mathrm{ac}-i} + c_{\mathrm{ac}-i}$ for *ac*-DGs and $C_{\mathrm{dc}-j}(P^{\mathrm{G}}_{\mathrm{dc}-j}) = a_{\mathrm{dc}-j}(P^{\mathrm{G}}_{\mathrm{dc}-j})^2 + b_{\mathrm{dc}-j}P^{\mathrm{G}}_{\mathrm{dc}-j} + c_{\mathrm{dc}-j}$ for *dc*-DGs), with parameters given in Table A3. The percentage of losses in the *ICs* and their operation limits are also given in Table A3.

The communication network of the HMG is shown in Fig. A2a, and the data is transferred among agents with a frequency of 100Hz. The numbered circles (i.e., "bus *dc*-j" and "bus *ac*-i") are showing the location, where the DG loads are connected. The adjacency matrix (**A**) describing the communication network is given by Fig. A2b. In this matrix, element $a_{ij} = 1$ if DG_i is communicating with DG_j; otherwise, $a_{ij} = 0$. Rows (and columns) 1 to 6 show the communication links of the *dc*-MG, while rows (and columns) 7 to 12 show the communication links of the *ac*-MG. Communication links of the *ICs* are shown in rows (and columns) 13 to 15.

The inner (voltage and current) control loops implemented in each DG and *IC* were defined depending on the nature of the controlled variables (*ac* or *dc*). Specifically, Proportional-resonant controllers were implemented for the *ac* controlled variables and proportional-integral controllers for the *dc* controlled variables. The inner controllers were tuned considering a bandwidth high enough to avoid coupling with the other control loops and to manage the transient changes in the secondary variables. However, since the main focus is the secondary control, the inner control level is considered out of the scope of this article.

The following approach was used for tuning the gains of the secondary controllers. First, all the controllers were considered active, full-load conditions were assumed with all the DGs and *ICs* working within limits. Second, the following parameters were sequentially tuned: (i) the parameters related to the local voltages/frequencies regulation ($k^a_{\mathrm{dc}-j}, k^a_{\mathrm{ac}-i}$), considering the other parameters are zero, (ii) the parameters associated with the incremental cost consensus within each MG ($k^b_{\mathrm{dc}-j}, k^b_{\mathrm{ac}-i}$), considering gains $k^a_{\mathrm{dc}-j}, k^a_{\mathrm{ac}-i}$ as tuned in (i), (iii) the parameters associated with the incremental cost consensus between MGs ($k^c_{\mathrm{dc}-j}, k^c_{\mathrm{ac}-i}, \tau^a_{\mathrm{IC}-k}$), with gains $k^{a,b}_{\mathrm{dc}-j}, k^{a,b}_{\mathrm{ac}-i}$ as tuned in (i) and (ii), (iv) the parameters corresponding to the λ^{IC} consensus ($\tau^b_{\mathrm{IC}-k}$), considering parameters tuned in (i), (ii) and (iii), and (v) the parameters corresponding to the operation limits constraints, by independently touching the operation limit of each unit.

TABLE A1
HYBRID *ac/dc*-MG, PARAMETERS OF THE LINES.

Line	Ω	Line	Ω	Line	Ω
R_{12}	0.67	R_{35}	0.94	$\mathbf{Z}^\dagger$	$0.10 + j0.79$
R_{13}	0.78	R_{46}	0.47	Z_{IC}	$0.08 + j2.01$
R_{34}	0.50	R_{IC}	0.10	$\mathbf{z}^\dagger = \{z_{13}, z_{24}, z_{34}, z_{46}, z_{56}\}$	

TABLE A2
HYBRID *ac/dc*-MG, PARAMETERS OF THE CONTROLLERS.

Param.	*dc*-DGs	
$k^a_{\mathrm{dc}-j}$	0.1	(1/s)
$k^{b,c}_{\mathrm{dc}-j}$	1.0	(1/s)
$k^{d,e}_{\mathrm{dc}-j}$	0.2	
$\mu^{a,b}_{\mathrm{dc}-j}$	2.5E-3	
$M_{\mathrm{dc}-i}$	-3E-3	(V/W)
Param.	***ICs***	
$1/\tau_{\mathrm{IC}}$	250.0	(1/W)
$\tau^a_{\mathrm{IC}}, \tau^b_{\mathrm{IC}}$	0.2	
$\mu^a_{\mathrm{IC}}, \mu^b_{\mathrm{IC}}$	2.5E-3	

Param.	*ac*-DGs	
$k^a_{\mathrm{ac}-i}$	0.1	(1/s)
$k^{b,c}_{\mathrm{ac}-i}$	0.1	(1/s)
$k^{d,e}_{\mathrm{ac}-i}$	0.2	
$\mu^{a,b}_{\mathrm{ac}-i}$	2.5E-3	
$M_{\mathrm{ac}-i}$	-2.1E-3	(rad/sW)
β_i	12.0	(1/s)
b_i	50.0	(V/s)
$N_{\mathrm{ac}-i}$	-1.8E-3	(V/VAr)
ω_c	12.566	(rad/s)

TABLE A3
DGS AND *ICs* PARAMETERS.

***ac*-DG$_i$**	**1**	**2**	**3**	**4**	**5**	**6**
$a_{\mathrm{ac}-i}(\$/kW^2)$	0.55	0.49	0.44	0.66	0.39	0.27
$b_{\mathrm{ac}-i}(\$/kW)$	1.5	2.4	2.3	1.9	2.9	3.2
$c_{\mathrm{ac}-i}(\$)$	70	60	55	67	43	76
$P^{\mathrm{G}+}_{\mathrm{ac}-i}(kW)$	3.0	3.0	3.0	3.0	3.0	3.0
$P^{\mathrm{G}-}_{\mathrm{ac}-i}(kW)$	0.0	0.0	0.0	0.0	0.0	0.0
***dc*-DG$_j$**	**7**	**8**	**9**	**10**	**11**	**12**
$a_{\mathrm{dc}-j}(\$/kW^2)$	0.31	0.52	0.46	0.51	0.21	0.79
$b_{\mathrm{dc}-j}(\$/kW)$	2.4	1.6	2.0	2.6	3.2	0.9
$c_{\mathrm{dc}-j}(\$)$	57	64	58	68	61	62
$P^{\mathrm{G}+}_{\mathrm{dc}-j}(kW)$	2.5	2.5	2.5	2.5	2.5	2.5
$P^{\mathrm{G}-}_{\mathrm{dc}-j}(kW)$	0.0	0.0	0.0	0.0	0.0	0.0
IC$_k$	**13**	**14**	**15**			
$k^{\mathrm{LOSS}}_k(\%)$	4.0	6.0	2.0			
$P^{\mathrm{ac}+}_{\mathrm{IC}-k}(kW)$	1.2	1.2	1.2			
$P^{\mathrm{ac}-}_{\mathrm{IC}-k}(kW)$	-1.2	-1.2	-1.2			

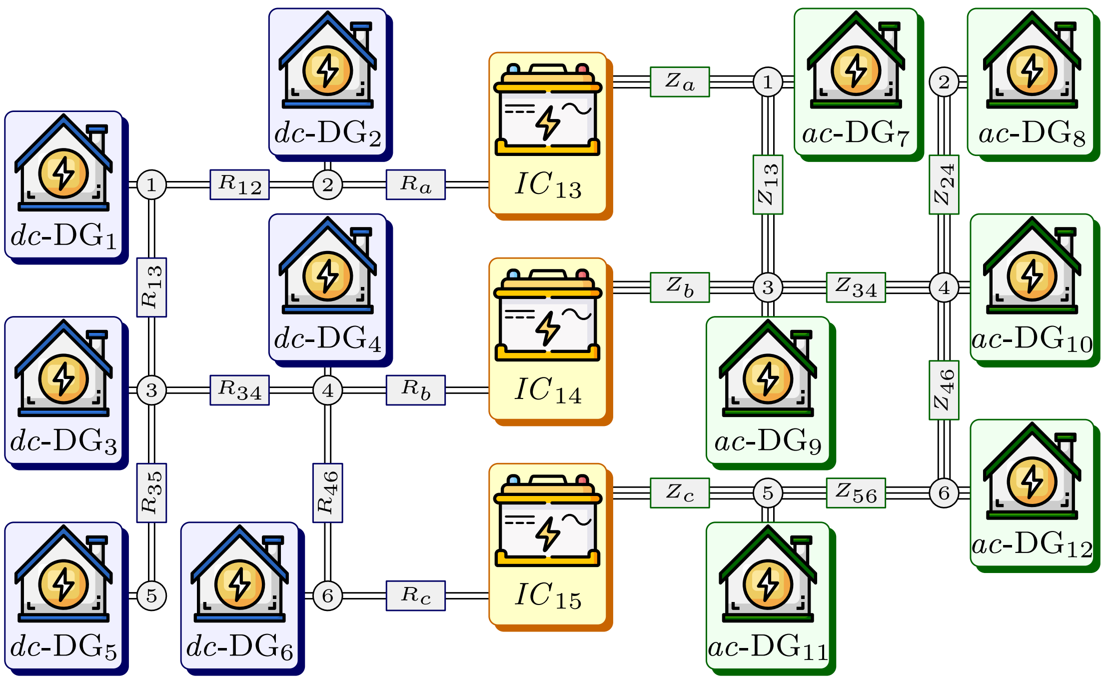

Fig. A1. Topology of the hybrid *ac/dc*-MG under study with multiple *ICs*.

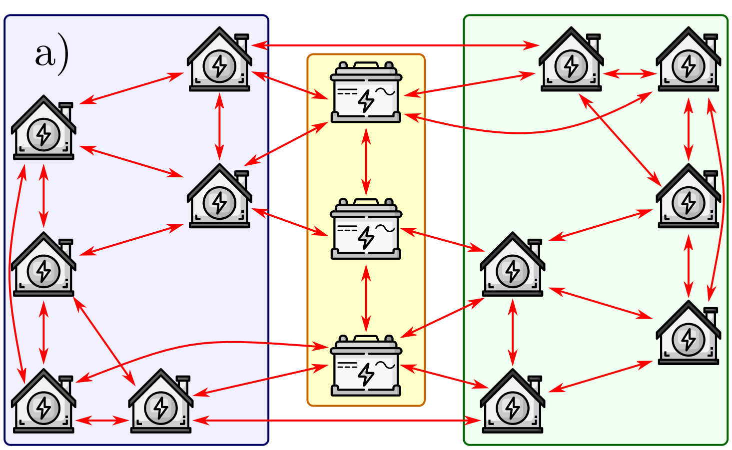

b)

$$
\mathbf{A} = \left(\begin{array}{cccccc:cccccc:ccc}
0&1&1&1&1&0&0&0&0&0&0&0&0&0&0\\
1&0&0&1&0&0&1&0&0&0&0&0&1&0&0\\
1&0&0&1&1&1&0&0&0&0&0&0&0&0&0\\
1&1&1&0&0&0&0&0&0&0&0&0&1&1&0\\
1&0&1&0&0&1&0&0&0&0&0&0&0&0&1\\
0&0&1&0&1&0&0&0&0&0&1&0&0&0&1\\
\hdashline
0&1&0&0&0&0&0&1&0&1&0&0&1&0&0\\
0&0&0&0&0&0&1&0&0&1&0&1&1&0&0\\
0&0&0&0&0&0&0&0&0&1&1&1&0&1&1\\
0&0&0&0&0&0&1&1&1&0&0&1&0&0&0\\
0&0&0&0&0&1&0&0&1&0&0&1&0&0&1\\
0&0&0&0&0&0&0&1&1&1&1&0&0&0&0\\
\hdashline
0&1&0&1&0&0&1&1&0&0&0&0&0&1&0\\
0&0&0&1&0&0&0&0&1&0&0&0&1&0&1\\
0&0&0&0&1&1&0&0&1&0&1&0&0&1&0
\end{array}\right)
$$

Fig. A2. The hybrid *ac/dc*-MG under study with multiple *ICs*. a) Communication network. b) Adjacency matrix.